Published in final edited form as:
Hum Brain Mapp. 2008 October ; 29(10): 1207–1214. doi:10.1002/hbm.20459.

Noninvasive Measurement of the Cerebral Blood Flow Response in Human Lateral Geniculate Nucleus With Arterial Spin Labeling fMRI

Kun Lu[1,2,*], **Joanna E. Perthen**[1,2], **Robert O. Duncan**[3], **Linda M. Zangwill**[3], and **Thomas T. Liu**[1,2]

[1]Center for Functional MRI, University of California San Diego, La Jolla, California

[2]Department of Radiology, University of California San Diego, La Jolla, California

[3]Hamilton Glaucoma Center, University of California San Diego, La Jolla, California

Abstract

To date, functional magnetic resonance imaging (fMRI) studies of the lateral geniculate nucleus (LGN) have primarily focused on measures of the blood oxygenation level dependent (BOLD) signal. Arterial spin labeling (ASL) is an MRI method that can provide direct measures of functional cerebral blood flow (CBF) changes. Because CBF is a well-defined physiological quantity that contributes to BOLD contrast, CBF measures can be used to improve the quantitative interpretation of fMRI studies. However, due in part to the low intrinsic signal-to-noise ratio of the ASL method, measures of functional CBF changes in the LGN are challenging and have not previously been reported. In this study, we demonstrate the feasibility of using ASL fMRI to measure the CBF response of the LGN to visual stimulation on a 3 T MRI system. The use of background suppression and physiological noise reduction techniques allowed reliable detection of LGN activation in all five subjects studied. The measured percent CBF response during activation ranged from 40 to 100%, assuming no interaction between the left and right LGN.

Keywords

lateral geniculate nucleus; arterial spin labeling; functional magnetic resonance imaging; background suppression; physiological noise reduction

Introduction

The lateral geniculate nucleus (LGN) is a subdivision of gray matter in the thalamus that is responsible for relaying visual information from the retina to the primary visual cortex. Noninvasive imaging of the LGN can provide important information to aid our understanding of the visual system in both healthy and diseased states. For example, neurodegeneration associated with primary open angle glaucoma is not restricted to the retinal ganglion cells, but rather extends to the target neurons in the LGN [Luthra et al., 2005; Yucel et al., 2000, 2001, 2003]. Studies of functional changes in the LGN may therefore aid in the detection and understanding of neurodegeneration in glaucoma.

*Correspondence to: Kun Lu, Ph.D., UCSD Center for Functional MRI, 9500 Gilman Drive, MC 0677, La Jolla, CA 92093-0677. kunlu@ucsd.edu.

Compared to visual cortex studies, functional imaging of the LGN is technically challenging because of the LGN's relatively small size (91–157 mm^3 [Andrews et al., 1997]) and subcortical location. Previous functional magnetic resonance imaging (fMRI) studies have used the blood oxygenation level dependent (BOLD) signal to measure functional activation in human LGN [Chen and Zhu, 2001; Chen et al., 1998a,b; Fujita et al., 2001; Kastner et al., 2004; Miki et al., 2001a,b, 2003, 2004, 2005; O'Connor et al., 2002] and to map the retinotopic organization of this structure [Chen et al., 1999; Schneider et al., 2004]. Although BOLD fMRI provides good sensitivity and spatial resolution, the quantitative interpretation of the BOLD signal is not always straightforward because of its complex dependence on a number of physiological variables, such as cerebral blood flow (CBF), the cerebral metabolic rate of oxygen, and cerebral blood volume [Buxton et al., 2004; Kwong et al., 1992; Ogawa et al., 1990]. Interpretation of the BOLD signal is especially problematic in clinical populations in which changes in the cerebrovascular system due to factors such as disease, medication, and age, can significantly alter the BOLD signal [Behzadi and Liu, 2005; D'Esposito et al., 2003].

Arterial spin labeling (ASL) is a noninvasive MRI method that can provide quantitative measures of CBF, which is a well-defined physiological quantity [Detre et al., 1992; Williams et al., 1992]. As compared to BOLD, measures of functional changes in CBF have been shown to exhibit less intersubject variability and to be more robust in the face of baseline vascular changes [Aguirre et al., 2002; Brown et al., 2003; Stefanovic et al., 2006; Tjandra et al., 2005; Wang et al., 2003]. It also has been suggested that the CBF signal may be more localized to brain parenchyma than BOLD [Kim, 1995; Luh et al., 2000]. In addition, CBF measures can be combined with BOLD measures to yield quantitative estimates of changes in oxidative metabolism [Davis et al., 1998; Hoge et al., 1999]. Although ASL has been widely applied to fMRI studies of the visual cortex, its application to the study of the LGN has not been previously reported, due in part to its low intrinsic signal-to-noise ratio (SNR) compared to BOLD. In a prior study from our laboratory, we showed that the use of retrospective physiological noise reduction methods can significantly improve the SNR of the ASL signal in the visual cortex and hippocampal region [Restom et al., 2006]. Background suppression methods have been shown to reduce the standard deviation of baseline ASL images, but their impact on the SNR of functional scans has not been well established [St Lawrence et al., 2005; Ye et al., 2000]. In this study, we show that the combination of physiological noise reduction and background suppression methods is critical for the robust detection of functional CBF activation in the LGN.

Human Subjects and Equipment

Five healthy adult subjects (two male) with normal vision, aged 25–40 years, participated in the study. Written informed consent was obtained according to an Institutional Review Board approval from the University of California, San Diego.

All experiments were performed using a General Electric 3.0-T EXCITE system, with an eight-channel receive-only head coil. Physiological (cardiac and respiratory) fluctuations were recorded using a pulse oximeter (INVIVO Magnitude 3150M patient monitor, Orlando, Florida) and a respiratory effort transducer (TSD201, BioPac Systems, Goleta, CA), respectively. The visual stimulus used in the study was generated using the Psychophysics Toolbox [Brainard, 1997; Pelli, 1997] for Matlab (Mathworks, Natick, MA) on a PowerBook G3 computer (Apple, Cupertino, CA), and was projected onto a back projection screen placed inside the scanner bore using an NEC Solutions (Itasca, IL) LT 157 liquid crystal display projector. The general specifications of the visual presentation system were as follows: viewing distance = 60 cm; field of view = 25° H × 18° V; maximum luminance = 28.9 cd/m^2; resolution = 1024 H × 768 V; 60-Hz refresh rate.

Experimental Protocol

Data Acquisition

Functional data were acquired using a quantitative pulsed ASL sequence (PICORE QUIPSS II) [Wong et al., 1998] with single-shot spiral readout. Five contiguous axial slices, each 5-mm thick, were acquired at the level of the LGN and primary visual cortex. A tagging slab of width 200 mm was placed 10 mm below the most inferior slice. The QUIPSS II parameters TI1 and TI2 were chosen to satisfy the following two criteria [Wong et al., 1998]: (1) TI1 is less than the natural temporal bolus width δ and (2) TI2-TI1 is greater than the longest transit delay Δt. We used measures of the ASL signal over a range of inversion times to estimate the bolus width and transit delays and determined that TI1 = 700 ms and TI2 = 1,400 ms were consistent with the QUIPSS II requirements [Buxton et al., 1998]. A total of 80 images (interleaved tag and control) per run were acquired. Other parameters were as follows: TE 3.2 ms, matrix size 64 × 64, FOV 22 cm, flip angle 90°, TR 3.0 s. Background suppression was used to reduce the static tissue components [Ye et al., 2000]. It consisted of a presaturation pulse train with two 90° windowed sinc pulses, with crusher gradients to saturate the imaging slab immediately prior to the application of the ASL tagging pulse and two adiabatic inversion pulses placed at 233 and 833 ms after the presaturation pulse train. The timing of the inversion pulses was optimized to achieve a theoretical attenuation of at least 95% in all imaging slices, assuming typical T1 values of 1,331, 832, and 3,900 ms at 3.0 T for gray matter, white matter, and CSF, respectively [Luh et al., 2000; Wansapura et al., 1999]. The number of inversion pulses was limited to 2 in order to minimize the losses in the perfusion signal because of the imperfections of the pulses and magnetization transfer effects [Garcia et al., 2005b; Talagala et al., 2004; Ye et al., 2000]. The remaining tissue signal component in the LGN area averaged among the five subjects after suppression was found experimentally to be 6, 10, and 12% in the LGN slices (slices 2, 3, and 4, respectively).

For each subject, two 4-min background-suppressed ASL runs were acquired. In addition to the background-suppressed ASL runs, two additional 4-min runs using the ASL sequence without background suppression were acquired. In these runs, a dual-echo single-shot spiral acquisition (TE = 3.2, 25 ms) was used. During all four functional experiments, cardiac and respiratory activities were recorded. A high-resolution structural scan was also acquired using an inversion-prepared fast spoiled gradient echo pulse sequence, with an inversion delay of 450 ms, 124 axial slices (1-mm thick), FOV 25 cm, matrix size 256 × 256, TR 7.9 ms, TE 3.1 ms, flip angle 12°, and bandwidth 31.25 kHz.

During each functional run, the subjects were instructed to passively view a visual stimulus with a central fixation point. The visual stimulus consisted of contrast-reversing (8 Hz) checkerboard patterns (100% contrast, 25° horizontal and 15° vertical aperture) that alternated between the left and right visual fields in a block design (left visual field first, 30 s left, 30 s right, a total of four repeats for each visual field, total time 4 min). The central fixation point (0.6°) was visible throughout the experiment.

Data Analysis

The first four images of each scan were excluded from data analysis to allow the MRI signal to reach steady state. All functional runs were motion-corrected and then registered to the first functional run using AFNI software [Cox, 1996]. The anatomical volume was registered to the functional volume with an in-house MATLAB program that utilizes the scanner coordinates of each volume. The accuracy of this registration program was verified on phantoms, using high-resolution interleaved spiral images obtained with the same spiral pulse sequence used for the functional studies. Functional CBF responses were computed from the surround subtraction of the control and tag image series in the background-suppressed data. If odd indices

correspond to control images and even indices correspond to tag images, then the surround subtraction over an image acquisition time series $y[n]$, $n = 0, 1, 2, \ldots$ produces the perfusion weighted time series: $\{y[1] - (y[0] + y[2])/2, (y[1] + y[3])/2 - y[2], \ldots\}$ [Liu and Wong, 2005]. Functional BOLD responses were computed from the running average (average of each image with the mean of its two nearest neighbors) of the second echo (TE = 25 ms) nonbackground-suppressed data [Liu and Wong, 2005]. CBF responses were also formed from the first echo (TE = 3 ms) of the nonbackground-suppressed data, but as shown in the Results section, the SNR of these data was too low to provide reliable detection of LGN activation, even after physiological noise correction.

Statistical analysis of the data was performed using a general linear model (GLM) approach for the analysis of ASL data [Restom et al., 2006]. The stimulus-related regressor in the GLM was assumed to be a vector, obtained by convolving the stimulus pattern with a gamma density function of the form $h(t) = (\tau n!)^{-1} ((t - \Delta t)/\tau)^n \exp(-(t - \Delta t)/\tau)$ for $t \geq \Delta t$ and 0 otherwise, with $\tau = 1.2$, $n = 3$, and $\Delta t = 1$ [Boynton et al., 1996]. The measured cardiac and respiratory fluctuation data were included in the GLM as regressors to model the physiological modulation of the ASL signal. In addition, a constant and a linear term were included as nuisance regressors. The data from the two runs (either two background suppressed or two nonbackground suppressed runs) were concatenated prior to analysis with an expanded GLM (cf. Eq. (10) in Restom et al. [2006]). As described in Restom et al. [2006], the expanded GLM allowed for different physiological and nuisance regressors for each run. The estimated physiological noise components were removed from the original data to form the noise-corrected CBF and BOLD time series. Probability values (P values) were calculated on a per-voxel basis using the methods described in Restom et al. [2006]. A Satterthwaite approximation was used to account for the noise covariance introduced by the ASL surround subtraction process [Kiebel et al., 2003; Restom et al., 2006; Worsley and Friston, 1995].

Because of the low SNR of the CBF measures, detection of functional CBF activation was confined to an anatomical region of interest (ROI) encompassing the LGN region. This ROI was defined on the structural images based on anatomical landmarks surrounding the LGN (the hippocampal formation and optical radiation [Fujita et al., 2001]). The size of the ROI (22–30 voxels per hemisphere) was chosen to be larger than the actual size of the LGN to allow for partial-voluming and image-blurring effects. A per-voxel threshold of $P < 0.008$ (corresponding to $P < 0.05$ after correction for multiple comparisons) with a nearest neighbor clustering criteria was used to define voxels with significant functional CBF activation. Correction for multiple comparisons was performed using the AFNI program AlphaSim [Cox, 1996; Forman et al., 1995; Xiong et al., 1995], with a minimum cluster size of two and in-plane full-width half maximum (FWHM) of 5.8 mm × 5.8 mm. To maintain the same P-value threshold across subjects, the largest ROI size (30 voxels) was used. Estimates of the FWHM were obtained from Bloch simulations of the spiral acquisition process with an assumed T2* = 30 ms, which was measured from the dual echo data.

For detection of BOLD activation, we used the same anatomical ROI and per-voxel threshold as for the functional CBF detection. In addition, to facilitate comparison with prior studies, we also considered a more stringent per-voxel threshold of $P < 0.0001$, corresponding to $P < 0.0005$ after correction for multiple comparisons within the anatomical ROI.

For each subject and each hemisphere, average CBF and BOLD time courses were obtained by averaging the individual noise-corrected time courses across activated CBF and BOLD voxels, respectively. Percent change CBF and BOLD responses were calculated by dividing the respective time course by its baseline, which is defined as the mean signal during the off period of the visual stimulus for each LGN.

The temporal variation of the perfusion measurements was assessed in the active voxels of the left and right LGN by calculating the standard deviation of the residual noise estimated from the GLM. Without physiological noise correction, the residual noise included the cardiac and respiratory induced variations; whereas with physiological noise correction, estimates of the cardiac and respiratory variations were removed from the residual noise. To compensate for the higher receiver gains used in the background suppressed runs, the standard deviations of the background suppressed residual noise components were scaled down by the relative difference in the receiver gains to achieve the same effective gain for all the noise terms.

Results

Bilateral CBF and BOLD activation within the LGN was detected in all subjects. Figure 1A shows an example CBF activation map from Subject 1, who demonstrated activation in both the left and right LGN and visual cortex. Figure 1B shows the CBF time courses averaged over the active CBF voxels for the left and right LGN. Both average time courses are highly correlated with their respective stimulus patterns ($r > 0.8$).

Table I summarizes the percent CBF and BOLD responses on a per subject basis. The percent change in CBF response ranged from 40 to 100%, with the exception of the response in Subject 5's left LGN, which had a physiologically unlikely percent CBF change (400%). An examination of Subject 5's data revealed a low CBF estimate during the baseline period in the left LGN area, as compared to the right LGN. The low baseline CBF estimate was in turn due to the presence of large negative values in the CBF time series during two out of the four baseline periods. As the CBF time course is obtained from the surround subtraction of the control and tag images, the presence of residual image noise components that are not removed by background suppression or physiological noise correction can give rise to anomalous negative values due to the differencing of the noise components.

The number of active CBF voxels per hemisphere ranged from two to four among the five subjects, corresponding to activation volumes of 118–236 mm^3. The measured activation volume here is similar to the previously reported BOLD-based activation volumes of 240 ± 29 mm^3 [Chen et al., 1999; Kastner et al., 2004], and agree reasonably with the reported anatomical volume 91–157 mm^3 [Andrews et al., 1997].

At a threshold of $P < 0.05$ (same as the threshold used for the CBF with correction for multiple comparisons), the measured percent BOLD response ranged from 0.47% to 0.97%, and the numbers of active BOLD voxels ranged from 2 to 14 corresponding to activation volumes of 118–826 mm^3. Overlap of the activated CBF and BOLD voxels was observed in all but two of the LGN (Table I). When using the lower corrected threshold of $P < 0.0005$, the detected number of active BOLD voxels ranged from 2 to 7 corresponding to LGN volumes of 118–413 mm^3, except in Subject 4's right LGN, where no BOLD activation was found. When using this lower threshold, overlap between the BOLD and CBF activation regions was found in only 4 of the 10 LGN.

Figure 2A compares the number of activated CBF voxels with and without the use of background suppression and physiological noise correction. In the absence of background suppression and physiological noise correction, no active LGN voxels were found in any of the five subjects. After applying physiological noise correction to the nonbackground-suppressed data, one subject showed discernable activation. With background suppression alone, two subjects showed significant activation. The use of both physiological noise correction and background suppression resulted in the largest improvement in the SNR of the ASL data, with the detection of LGN activation in all five subjects. Figure 2B compares the standard deviation of the residual noise component of the GLM in the LGN voxels with and

without the use of background suppression and physiological noise correction. A reduction of 61–75% in the standard deviation was observed after background suppression. Applying physiological noise correction to the background suppressed data provided an additional reduction of 6–18%. The combination of the two methods reduced the standard deviation of the residual noise by 75–89% in the five subjects.

Discussion

We have shown that CBF activation within the LGN can be measured using ASL fMRI. To our knowledge, this is the first quantitative measure of the functional CBF response in the human LGN. Despite the SNR gains achieved with the use of physiological noise reduction and background suppression methods, ASL is still an inherently low SNR technique and necessitates the use of larger voxels than those typically used in BOLD fMRI studies. The voxel size used here (3.44 mm × 3.44 mm × 5 mm) was chosen after performing preliminary experiments with slice thicknesses of 3 and 4 mm, but the SNR using these smaller voxels was too low to provide robust detection of CBF activation in the LGN. The use of large voxels is likely to have caused underestimation of the percentage signal change during activation. Indeed, the measured BOLD percent change of 0.47%–0.97% is smaller than the 1.2% measured by Kastner et al. [2004] at 3 T using 3.17 mm × 3.17 mm × 3.0 mm voxels. Other recently published reports indicate percent BOLD changes of 1.63%–3.09% at 1.5 T for 3.17 mm × 3.17 mm × 3 mm voxels [Fujita et al., 2001] and 2.2% at 4 T for 1.56 mm × 1.56 mm × 3 mm voxels [Chen et al., 1999].

When using the same threshold (per-voxel $P < 0.008$ corresponding to $P < 0.05$ after correction for multiple comparisons) to detect active CBF and BOLD voxels, the number of active BOLD voxels (2–14) was greater than the number of active CBF voxels (2–4), reflecting in part the lower SNR of the CBF measures. Both the per-voxel and corrected *P*-values are higher than the corresponding *P*-values used in prior BOLD studies of the LGN. The use of a higher corrected threshold and a relatively small anatomical ROI in this study was motivated by the low SNR of the CBF measures. The thresholds used in prior BOLD studies have varied greatly depending on the study design and magnetic field strength, with corrected *P*-values of 6×10^{-4} at 4 T, 0.01 at 3 T, and 0.05 at 1.5 T [Chen et al., 1998b, 1999; Fujita et al., 2001; Kastner et al., 2004]. In addition, as compared to the current study, the prior studies used a larger ROI (typically 1,000–2,000 voxels) when correcting for multiple comparisons, resulting in larger relative differences between the corrected and per-voxel thresholds. Because of the higher thresholds used in this study, we found that the number of active BOLD voxels was greater than the previously reported values. When the corrected threshold in this study was reduced to 0.0005, the per-voxel threshold decreased to a value of 0.0001, which is roughly comparable to the reported per-voxel threshold of 0.0002 used by Chen et al. [1999]. At this lower threshold, the measured BOLD activation volume (118–413 mm^3) was found to be comparable to previously reported values [Chen et al., 1998b, 1999; Fujita et al., 2001; Kastner et al., 2004].

A comparison of the active BOLD and CBF regions showed a partial overlap of the two regions, with the CBF region typically confined to the parenchyma of the thalamus, whereas the BOLD region consistently extended toward the lateral–inferior or posterior–inferior edge of the thalamus. In addition, the amount of overlap decreased as the threshold on the BOLD activation became more stringent. These findings are consistent with those of a previous study of motor cortex activation by Luh et al. [2000], which concluded that the CBF signal is primarily localized to the brain parenchyma, whereas the BOLD signal is more weighted to the venous compartment.

Our results indicate that background suppression and physiological noise correction are critical for the detection of functional CBF changes in the LGN. The reduction of noise components

(e.g. due to respiration-induced motion and magnetic field fluctuations) with background suppression was sufficient to allow for detection of activation in Subjects 1 and 2, who exhibited smaller residual noise levels prior to suppression. For Subjects 3 through 5, who exhibited higher initial residual noise levels, the combination of background suppression and physiological noise correction was necessary to reduce the residual noise to levels that allowed for detection of activation. The further reduction of the residual noise by applying physiological noise correction to the background suppressed data most likely reflects the presence of fluctuations in the CBF signal, such as respiratory modulation of CBF through changes in carbon dioxide [Wise et al., 2004] and cardiac modulations of the tag bolus (discussed later and in Wu and Wong [2006]). Since these factors directly affect the CBF signal, they are unlikely to be reduced by the attenuation of the static tissue component that is achieved by background suppression. Our results also indicate that even with the application of background suppression and physiological noise reduction methods the SNR of the CBF measures is still significantly lower than that of the BOLD measures. Other methods, such as single-shot 3D acquisitions [Gunther et al., 2005; Talagala et al., 2004], may prove to be useful for attaining further SNR increases for functional CBF measures. In addition, Wu et al. [2007] recently demonstrated that pseudocontinuous ASL [Garcia et al., 2005a] with optimized parameters offers higher tagging efficiency and SNR than pulsed ASL for baseline CBF measures. Further studies to determine whether pseudocontinuous ASL can provide better detection of functional CBF changes in the LGN would be useful.

It has been recently demonstrated that the CBF signal measured with a PICORE QUIPSS II ASL acquisition depends on the relative position of the tag and QUIPSS II saturation pulses within the cardiac cycle [Wu and Wong, 2006]. The observed dependence most likely reflects variations in the size of the tagged bolus created by the QUIPSS II approach because of cardiac-induced variations in blood velocity. The resultant variability in the CBF signal can be reduced by using cardiac gating of the sequence. However, because the acquisition is no longer synchronized with the stimulus, the gains achieved may be offset by decreases in statistical power because of the need to resample the data. Further work comparing the relative advantages of cardiac gating versus physiological noise correction would be useful. Alternatively, the use of a longer TI1 parameter in the order of about 1 s would decrease the sensitivity of the bolus size to cardiac fluctuations. However, the use of a longer TI1 parameter would be inconsistent with the QUIPSS II requirements for CBF quantification (see Data Acquisition section). In future work, it would be useful to determine whether a continuous ASL approach with a tagging duration of ~1 s could provide better performance than the pulsed ASL approach used here.

In this study, the baseline CBF in each LGN was estimated by averaging the signal measured during the off period (e.g. lack of hemispheric stimulus) for that LGN. This analysis implicitly assumes that the left and right LGN do not interact with each other during activation, e.g. an increase in CBF in one LGN will not affect CBF in the other. Departures from this assumption can cause bias in the estimates of baseline CBF, which in turn lead to bias in the estimates of the percent change in CBF. In future studies, the inclusion of control periods during which neither LGN is stimulated would be useful for minimizing these potential biases.

The present study is an initial demonstration of the feasibility of detecting functional CBF responses in the LGN with ASL fMRI. Because CBF is a fundamental physiological quantity, measures of functional CBF in the LGN may prove useful for furthering our understanding of neurode-generative diseases of the visual system such as glaucoma. Additional studies to refine the performance of ASL methods and demonstrate their application in clinical populations would be useful.

Acknowledgments

Contract grant sponsor: NIH; Contract grant number: 5R01EY011008-10

References

Aguirre GK, Detre JA, Zarahn E, Alsop DC. Experimental design and the relative sensitivity of BOLD and perfusion fMRI. Neuroimage 2002;15:488–500. [PubMed: 11848692]

Andrews TJ, Halpern SD, Purves D. Correlated size variations in human visual cortex, lateral geniculate nucleus, and optic tract. J Neurosci 1997;17:2859–2868. [PubMed: 9092607]

Behzadi Y, Liu TT. An arteriolar compliance model of the cerebral blood flow response to neural stimulus. Neuroimage 2005;25:1100–1111. [PubMed: 15850728]

Boynton GM, Engel SA, Glover GH, Heeger DJ. Linear systems analysis of functional magnetic resonance imaging in human V1. J Neurosci 1996;16:4207–4221. [PubMed: 8753882]

Brainard DH. The psychophysics toolbox. Spatial Vis 1997;10:433–436.

Brown GG, Eyler Zorrilla LT, Georgy B, Kindermann SS, Wong EC, Buxton RB. BOLD and perfusion response to finger-thumb apposition after acetazolamide administration: Differential relationship to global perfusion. J Cereb Blood Flow Metab 2003;23:829–837. [PubMed: 12843786]

Buxton RB, Frank LR, Wong EC, Siewert B, Warach S, Edelman RR. A general kinetic model for quantitative perfusion imaging with arterial spin labeling. Magn Reson Med 1998;40:383–396. [PubMed: 9727941]

Buxton RB, Uludag K, Dubowitz DJ, Liu TT. Modeling the hemodynamic response to brain activation. Neuroimage 2004;23(Suppl 1):S220–S233. [PubMed: 15501093]

Chen W, Zhu XH. Correlation of activation sizes between lateral geniculate nucleus and primary visual cortex in humans. Magn Reson Med 2001;45:202–205. [PubMed: 11180426]

Chen W, Kato T, Zhu XH, Ogawa S, Tank DW, Ugurbil K. Human primary visual cortex and lateral geniculate nucleus activation during visual imagery. Neuroreport 1998a;9:3669–3674. [PubMed: 9858377]

Chen W, Kato T, Zhu XH, Strupp J, Ogawa S, Ugurbil K. Mapping of lateral geniculate nucleus activation during visual stimulation in human brain using fMRI. Magn Reson Med 1998b;39:89–96. [PubMed: 9438442]

Chen W, Zhu XH, Thulborn KR, Ugurbil K. Retinotopic mapping of lateral geniculate nucleus in humans using functional magnetic resonance imaging. Proc Natl Acad Sci USA 1999;96:2430–2434. [PubMed: 10051659]

Cox RW. AFNI: Software for analysis and visualization of functional magnetic resonance neuroimages. Comput Biomed Res 1996;29:162–173. [PubMed: 8812068]

Davis TL, Kwong KK, Weisskoff RM, Rosen BR. Calibrated functional MRI: Mapping the dynamics of oxidative metabolism. Proc Natl Acad Sci USA 1998;95:1834–1839. [PubMed: 9465103]

D'Esposito M, Deouell LY, Gazzaley A. Alterations in the BOLD fMRI signal with ageing and disease: A challenge for neuroimaging. Nat Rev Neurosci 2003;4:863–872. [PubMed: 14595398]

Detre JA, Leigh JS, Williams DS, Koretsky AP. Perfusion imaging. Magn Reson Med 1992;23:37–45. [PubMed: 1734182]

Forman SD, Cohen JD, Fitzgerald M, Eddy WF, Mintun MA, Noll DC. Improved assessment of significant activation in functional magnetic resonance imaging (fMRI): Use of a cluster-size threshold. Magn Reson Med 1995;33:636–647. [PubMed: 7596267]

Fujita N, Tanaka H, Takanashi M, Hirabuki N, Abe K, Yoshimura H, Nakamura H. Lateral geniculate nucleus: Anatomic and functional identification by use of MR imaging. AJNR Am J Neuroradiol 2001;22:1719–1726. [PubMed: 11673167]

Garcia, DM.; de Bazelaire, C.; Alsop, DC. Pseudo-continuous flow driven adiabatic inversion for arterial spin labeling. Proceedings of the 13th Scientific Meeting of the Int Soc Magn Reson Med; 2005a. p. 37

Garcia DM, Duhamel G, Alsop DC. Efficiency of inversion pulses for background suppressed arterial spin labeling. Magn Reson Med 2005b;54:366–372. [PubMed: 16032674]

Gunther M, Oshio K, Feinberg DA. Single-shot 3D imaging techniques improve arterial spin labeling perfusion measurements. Magn Reson Med 2005;54:491–498. [PubMed: 16032686]

Hoge RD, Atkinson J, Gill B, Crelier GR, Marrett S, Pike GB. Investigation of BOLD signal dependence on cerebral blood flow and oxygen consumption: The deoxyhemoglobin dilution model. Magn Reson Med 1999;42:849–863. [PubMed: 10542343]

Kastner S, O'Connor DH, Fukui MM, Fehd HM, Herwig U, Pinsk MA. Functional imaging of the human lateral geniculate nucleus and pulvinar. J Neurophysiol 2004;91:438–448. [PubMed: 13679404]

Kiebel SJ, Glaser DE, Friston KJ. A heuristic for the degrees of freedom of statistics based on multiple variance parameters. Neuroimage 2003;20:591–600. [PubMed: 14527620]

Kim SG. Quantification of relative cerebral blood flow change by flow-sensitive alternating inversion recovery (FAIR) technique: Application to functional mapping. Magn Reson Med 1995;34:293–301. [PubMed: 7500865]

Kwong KK, Belliveau JW, Chesler DA, Goldberg IE, Weisskoff RM, Poncelet BP, Kennedy DN, Hoppel BE, Cohen MS, Turner R, et al. Dynamic magnetic resonance imaging of human brain activity during primary sensory stimulation. Proc Natl Acad Sci USA 1992;89:5675–5679. [PubMed: 1608978]

Liu TT, Wong EC. A signal processing model for arterial spin labeling functional MRI. Neuroimage 2005;24:207–215. [PubMed: 15588612]

Luh WM, Wong EC, Bandettini PA, Ward BD, Hyde JS. Comparison of simultaneously measured perfusion and BOLD signal increases during brain activation with T(1)-based tissue identification. Magn Reson Med 2000;44:137–143. [PubMed: 10893532]

Luthra A, Gupta N, Kaufman PL, Weinreb RN, Yucel YH. Oxidative injury by peroxynitrite in neural and vascular tissue of the lateral geniculate nucleus in experimental glaucoma. Exp Eye Res 2005;80:43–49. [PubMed: 15652525]

Miki A, Liu GT, Englander SA, van Erp TG, Bonhomme GR, Aleman DO, Liu CS, Haselgrove JC. Functional magnetic resonance imaging of eye dominance at 4 tesla. Ophthalmic Res 2001a;33:276–282. [PubMed: 11586061]

Miki A, Liu GT, Raz J, Englander SA, Bonhomme GR, Aleman DO, Modestino EJ, Liu CS, Haselgrove JC. Visual activation in functional magnetic resonance imaging at very high field (4 Tesla). J Neuroophthalmol 2001b;21:8–11. [PubMed: 11315986]

Miki A, Liu GT, Goldsmith ZG, Liu CS, Haselgrove JC. Decreased activation of the lateral geniculate nucleus in a patient with anisometropic amblyopia demonstrated by functional magnetic resonance imaging. Ophthalmologica 2003;217:365–369. [PubMed: 12913328]

Miki A, Liu CS, Liu GT. Effects of voxel size on detection of lateral geniculate nucleus activation in functional magnetic resonance imaging. Jpn J Ophthalmol 2004;48:558–564. [PubMed: 15592780]

Miki A, Liu GT, Modestino EJ, Bonhomme GR, Liu CS, Haselgrove JC. Decreased lateral geniculate nucleus activation in retrogeniculate hemianopia demonstrated by functional magnetic resonance imaging at 4 Tesla. Ophthalmologica 2005;219:11–15. [PubMed: 15627821]

O'Connor DH, Fukui MM, Pinsk MA, Kastner S. Attention modulates responses in the human lateral geniculate nucleus. Nat Neurosci 2002;5:1203–1209. [PubMed: 12379861]

Ogawa S, Lee TM, Kay AR, Tank DW. Brain magnetic resonance imaging with contrast dependent on blood oxygenation. Proc Natl Acad Sci USA 1990;87:9868–9872. [PubMed: 2124706]

Pelli DG. The VideoToolbox software for visual psychophysics: Transforming numbers into movies. Spat Vis 1997;10:437–442. [PubMed: 9176953]

Restom K, Behzadi Y, Liu TT. Physiological noise reduction for arterial spin labeling functional MRI. Neuroimage 2006;31:1104–1115. [PubMed: 16533609]

Schneider KA, Richter MC, Kastner S. Retinotopic organization and functional subdivisions of the human lateral geniculate nucleus: A high-resolution functional magnetic resonance imaging study. J Neurosci 2004;24:8975–8985. [PubMed: 15483116]

St Lawrence KS, Frank JA, Bandettini PA, Ye FQ. Noise reduction in multi-slice arterial spin tagging imaging. Magn Reson Med 2005;53:735–738. [PubMed: 15723412]

Stefanovic B, Warnking JM, Rylander KM, Pike GB. The effect of global cerebral vasodilation on focal activation hemodynamics. Neuroimage 2006;30:726–734. [PubMed: 16337135]

Talagala SL, Ye FQ, Ledden PJ, Chesnick S. Whole-brain 3D perfusion MRI at 3.0 T using CASL with a separate labeling coil. Magn Reson Med 2004;52:131–140. [PubMed: 15236376]

Tjandra T, Brooks JC, Figueiredo P, Wise R, Matthews PM, Tracey I. Quantitative assessment of the reproducibility of functional activation measured with BOLD and MR perfusion imaging: Implications for clinical trial design. Neuroimage 2005;27:393–401. [PubMed: 15921936]

Wang J, Aguirre GK, Kimberg DY, Roc AC, Li L, Detre JA. Arterial spin labeling perfusion fMRI with very low task frequency. Magn Reson Med 2003;49:796–802. [PubMed: 12704760]

Wansapura JP, Holland SK, Dunn RS, Ball WS Jr. NMR relaxation times in the human brain at 3.0 tesla. J Magn Reson Imaging 1999;9:531–538. [PubMed: 10232510]

Williams DS, Detre JA, Leigh JS, Koretsky AP. Magnetic resonance imaging of perfusion using spin inversion of arterial water. Proc Natl Acad Sci USA 1992;89:212–216. [PubMed: 1729691]

Wise RG, Ide K, Poulin MJ, Tracey I. Resting fluctuations in arterial carbon dioxide induce significant low frequency variations in BOLD signal. Neuroimage 2004;21:1652–1664. [PubMed: 15050588]

Wong EC, Buxton RB, Frank LR. Quantitative imaging of perfusion using a single subtraction (QUIPSS and QUIPSS II). Magn Reson Med 1998;39:702–708. [PubMed: 9581600]

Worsley KJ, Friston KJ. Analysis of fMRI time-series revisited again. Neuroimage 1995;2:173–181. [PubMed: 9343600]

Wu, WC.; Wong, EC. The effect of cardiac pulsation on fMRI data analysis. Proceedings of the 14th Scientific Meeting of the Int Soc Mag Reson Med; 2006. p. 1092

Wu WC, Fernandez-Seara M, Wehrli F, Detre J, Wang J. A theoretical and experimental investigation of the tagging efficiency of pseudo-continuous arterial spin labeling. Proceedings of the Int Soc Magn Reson Med 2007:375.

Xiong J, Gao JH, Lancaster JL, Fox PT. Clustered pixels analysis for functional MRI activation studies for the human brain. Hum Brain Mapp 1995;3:287–301.

Ye FQ, Frank JA, Weinberger DR, McLaughlin AC. Noise reduction in 3D perfusion imaging by attenuating the static signal in arterial spin tagging (ASSIST). Magn Reson Med 2000;44:92–100. [PubMed: 10893526]

Yucel YH, Zhang Q, Gupta N, Kaufman PL, Weinreb RN. Loss of neurons in magnocellular and parvocellular layers of the lateral geniculate nucleus in glaucoma. Arch Ophthalmol 2000;118:378–384. [PubMed: 10721961]

Yucel YH, Zhang Q, Weinreb RN, Kaufman PL, Gupta N. Atrophy of relay neurons in magno- and parvocellular layers in the lateral geniculate nucleus in experimental glaucoma. Invest Ophthalmol Vis Sci 2001;42:3216–3222. [PubMed: 11726625]

Yucel YH, Zhang Q, Weinreb RN, Kaufman PL, Gupta N. Effects of retinal ganglion cell loss on magno-, parvo-, koniocellular pathways in the lateral geniculate nucleus and visual cortex in glaucoma. Prog Retin Eye Res 2003;22:465–481. [PubMed: 12742392]

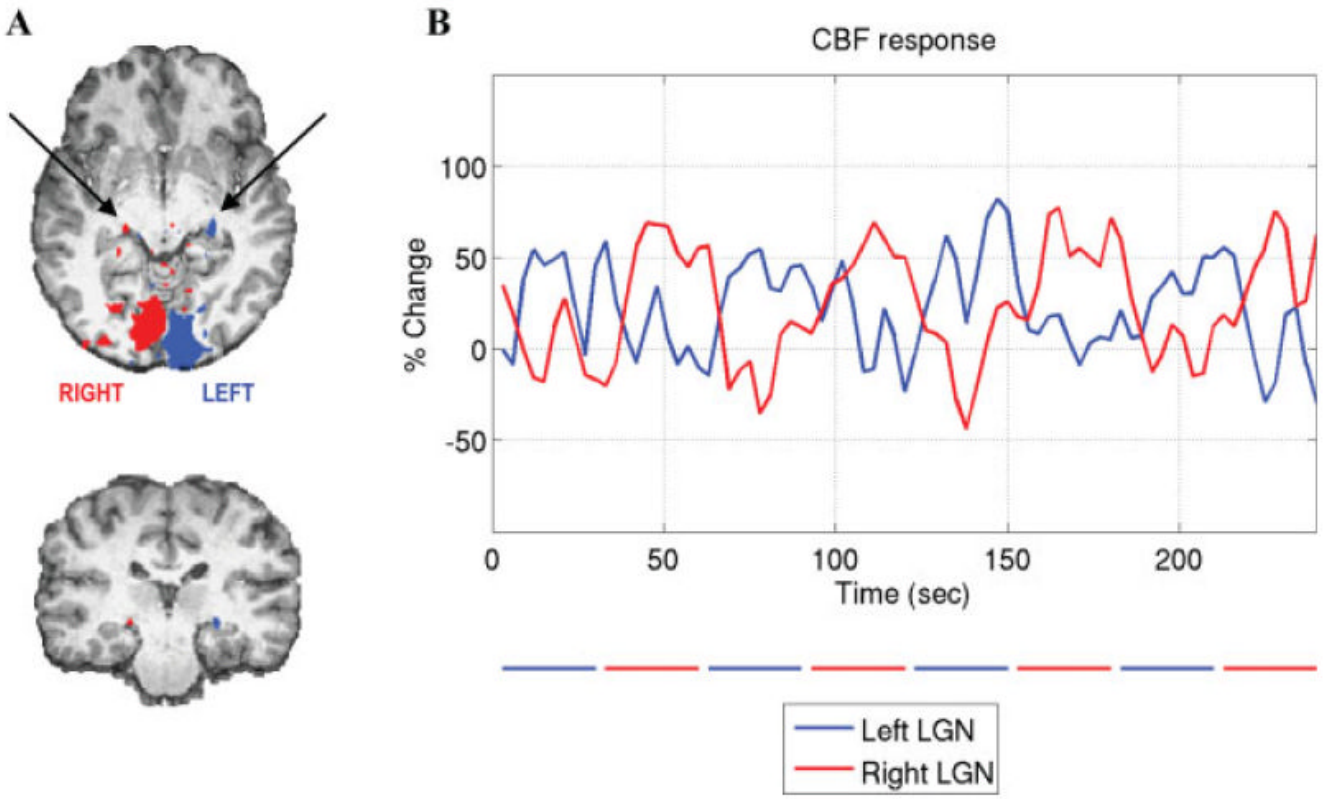

Figure 1.

A: Subject 1's CBF activation map ($P < 0.05$ corrected for multiple comparisons) superimposed on the anatomical image. Activation within the primary visual cortex and the LGN (indicated by the arrows) can be seen. **B**: CBF time courses averaged over active voxels within the left (blue) and right (red) LGN functional ROIs. The blue and red bars below the graph indicate the periods of visual stimulation presented to the contralateral visual fields. [Color figure can be viewed in the online issue, which is available at www.interscience.wiley.com.]

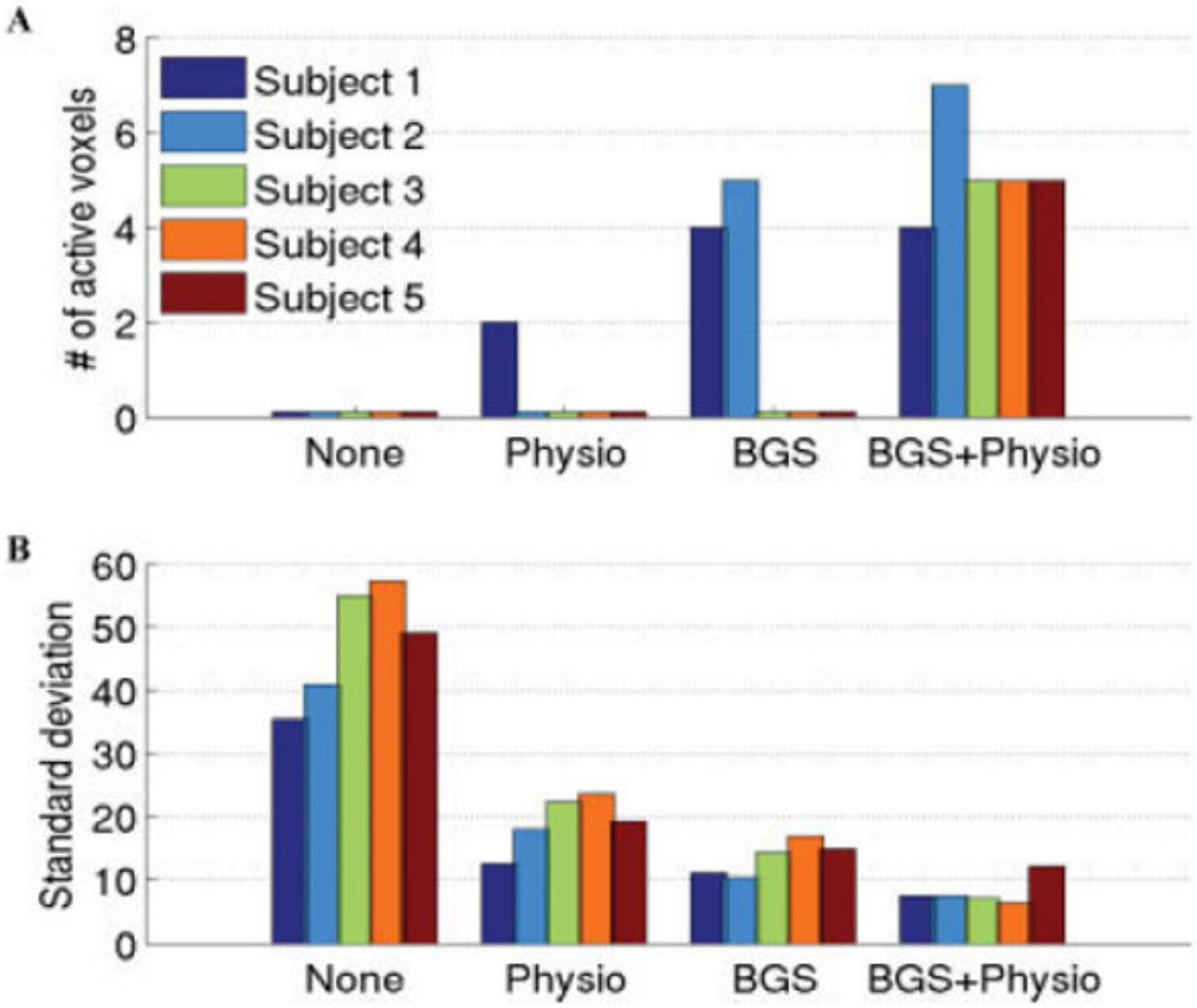

Figure 2.

A: Number of activated voxels detected in each subject (sum of the left and right LGN voxels) and **B**: Standard deviation of the estimated residual noise in LGN voxels when no correction methods were applied (first group on left), only physiological noise reduction was applied (2nd group), only background suppression (BGS) was applied (3rd group), and both physiological noise reduction and BGS were applied (4th group). The largest improvement in the sensitivity of the detection occurred when both BGS and physiological noise reduction were used. A value lower than 1 in (A) indicates no active voxels were found. [Color figure can be viewed in the online issue, which is available at www.interscience.wiley.com.]

Table I

Summary of the measured CBF and BOLD responses during LGN activation

Subject no.		CBF ($P < 0.05$)		BOLD ($P < 0.05$)			BOLD ($P < 0.0005$)		
		No. of voxels	% change	No. of voxels	% change	Overlap with CBF (no. of voxels)	No. of voxels	% change	Overlap with CBF (no. of voxels)
1	L	2	62	6	0.66	2	4	0.54	1
	R	2	48	7	0.52	1	3	0.80	1
2	L	3	68	14	0.68	3	7	0.84	2
	R	4	82	5	0.50	1	2	0.40	0
3	L	3	100	9	0.49	2	3	0.62	0
	R	2	89	4	0.90	1	3	0.70	0
4	L	3	40	4	0.48	1	2	0.40	1
	R	2	74	2	0.47	0	0	n/a	0
5	L	2	400[a]	5	0.86	1	3	0.99	0
	R	3	59	3	0.97	0	3	0.97	0

L, left LGN; R, right LGN.

[a] This large percent CBF increase is discussed further in the text.